HHS Public Access

Author manuscript

Biochem J. Author manuscript; available in PMC 2015 August 26.

Published in final edited form as:

Biochem J. 2015 June 15; 468(3): 435–447. doi:10.1042/BJ20150168.

Depletion of the Polyamines Spermidine and Spermine by Overexpression of Spermidine/spermine N^1-Acetyltransferase1 (SAT1) Leads to Mitochondria-Mediated Apoptosis in Mammalian Cells

Swati Mandal[a], **Ajeet Mandal**[a], and **Myung Hee Park**[a,1]

[a]Oral and Pharyngeal Cancer Branch, NIDCR, National Institutes of Health, Bethesda, MD, 20892, USA

Abstract

The polyamines putrescine, spermidine and spermine are intimately involved in the regulation of cellular growth and viability. Transduction of HEK293T cells with an adenovirus (AdSAT1) encoding a key polyamine catabolic enzyme, spermidine/spermine N^1-acetyltransferase1 (SAT1), leads to a rapid depletion of spermidine and spermine, arrest in cell growth and a decline in cell viability. Annexin V/ propidium iodide Fluorescent Activated Cell Sorter (FACS) analyses, Terminal Uridine Nucleotide End- Labeling (TUNEL) and caspase 3 assays showed a clear indication of apoptosis in AdSAT1 transduced cells (at 24–72 h), but not in cells transduced with GFP-encoding adenovirus (AdGFP). Apoptosis in the polyamine-depleted cells occurs by the mitochondrial intrinsic pathway, as evidenced by loss of mitochondrial membrane potential, increase in proapoptotic Bax, decrease in anti-apoptotic Bcl-xl, Bcl2, and Mcl-1 and release of cytochrome c from mitochondria, upon transduction with AdSAT1. Moreover, transmission electron microscopy images of AdSAT1-transduced cells revealed morphological changes commonly associated with apoptosis, including cell shrinkage, nuclear fragmentation, mitochondrial alteration, vacuolization and membrane blebbing. The apoptosis appears to result largely from depletion of the polyamines, spermidine and spermine, as polyamine analogs, α-methylspermidine and N^1,N^{12}-dimethylspermine that are not substrates for SAT1 could partially restore growth and prevent apoptosis of AdSAT1-transduced cells. Inhibition of polyamine oxidases did not restore the growth of AdSAT1-transduced cells or block apoptosis, suggesting that the growth arrest and apoptosis were not induced by oxidative stress resulting from accelerated polyamine catabolism. Taken together, these data provide strong evidence that the depletion of polyamines spermidine and spermine leads to mitochondria-mediated apoptosis.

[1]To whom correspondence should be addressed: Myung Hee Park, OPCB, Bldg 30 Rm 3A300, NIDCR, NIH, 30 Convent Drive Bethesda MD 20892-4340. Telephone: 301-496-5056, Fax number: 301-402-0823, mhpark@nih.gov.

AUTHOR CONTRIBUTION

Swati Mandal and Ajeet Mandal performed and analysed the data. Swati Mandal and Myung Hee Park designed the research, analysed the data and wrote the paper.

Keywords

Polyamine; spermidine; spermine; acetyltransferase; electron microscopy (EM); mitochondrial apoptosis

INTRODUCTION

The polyamines, putrescine, spermidine and spermine, are essential cellular constituents that are important in cell proliferation, transformation, differentiation, regulation of ion channels and the stabilization of important cellular components such as cell membranes and chromatin structures [1–4]. Cellular polyamine homeostasis is tightly maintained by intricate regulation at multiple levels, *i.e.* biosynthesis, catabolism and transport. Deregulation of polyamine metabolism is associated with various pathological conditions, including cancer. The polyamine pathways have been explored as targets for cancer chemotherapy and chemoprevention [5–7]. One well defined function of polyamines in eukaryotes is the requirement of spermidine as a precursor for hypusine modification in eukaryotic translation initiation factor, eIF5A (see a review, [8]. Independent of this role, the polyamines spermidine and spermine, as polycations, are required for protein synthesis and proliferation in mammalian cells [1–4, 9]

Polyamines have been implicated in apoptotic cell death in numerous reports in which the cellular polyamines were altered either by overexpression or by inhibition of biosynthetic enzymes (see a review [10]) and from studies with cells or animals genetically modified in polyamine pathways. Either excessive accumulation, or depletion, of cellular polyamines is deleterious to mammalian cells and can lead to cell death. Polyamines may act as facilitating or impeding factors of apoptosis depending on the concentration and the specific system. Concerning the potential mechanisms of their anti-apoptotic effects, it has been reported that polyamine binding to DNA protects against DNA cleavage from ionizing radiation [11] or that polyamines act as scavengers of reactive oxygen radicals [12]. On the other hand, excessive polyamines or activation of amine oxidation [by diamine oxidase, acetylpolyamine oxidase (APAO) or spermine oxidase (SMO)] can also cause oxidative stress and apoptosis by generation of H_2O_2 and reactive aldehydes intracellularly or extracellularly [2, 13, 14].

α-Difluoromethylornithine (DFMO), an irreversible inhibitor of ornithine decarboxylase (ODC), has been most widely used as a tool to elucidate polyamine function and also to control aberrant cell growth in cancer therapy and chemoprevention [5, 6]. Reduction of cellular polyamines, using DFMO, alone or in combination with other inhibitors of polyamine biosynthesis, induced apoptosis in a number of mammalian cell lines [15–18]. However, DFMO depletes cellular putrescine and spermidine, but not spermine, and the effects of DFMO are variable in different systems. In rat intestinal epithelial cells and the IEC-6 cell line, DFMO protected cells from apoptosis induced by tumour necrosis factor-α (TNF-α or camptothecin [19–21]. In this regard, major inconsistences exist in the literature regarding the role of polyamines in apoptosis, due to the complexities of polyamine actions and of apoptotic processes.

The cellular functions of polyamines have also been assessed by induction of the polyamine catabolic enzyme, SAT1 [22]. It catalyzes acetylation of spermidine or spermine to generate N^1-acetylspermidine, N^1-acetylspermine or N^1, N^{12}-diacetylspermine, which, in turn, are oxidatively degraded by acetylpolyamine oxidase (APAO) to N-acetylaminopropanal and a lower polyamine. However, previous attempts to deplete polyamines by overexpressing SAT1 [23–26] often did not achieve extensive depletion of spermidine and spermine, nor total inhibition of cell growth [7]. Very effective depletion of cellular polyamines has been accomplished by the use of bis-ethylated polyamine analogs, such as N^1, N^{11}-bis(ethyl)norspermine (BENSpm) [2]. This analog strongly induces SAT1 and SMO while suppressing polyamine biosynthetic enzymes ODC and adenosylmethionine decarboxylase (AdoMetDC), thereby it replaces natural polyamines putrescine, spermidine and spermine. Although BENSpm has been a valuable tool for the study of polyamine function and also as a potential anticancer agent, the fact that this analog could exert side effects as a polyamine agonist as well as an anti-agonist complicates the interpretation of its cellular effects. Thus, addressing the precise mechanisms of polyamine actions in cell growth and death has been hampered, partly because of the lack of effective means of depleting both polyamines spermidine and spermine, without introducing a polyamine analog.

Recently, the use of a SAT1 adenovirus enabled us to effectively and extensively deplete both spermidine and spermine in HEK293T cells [9] and to examine the primary effects of polyamine depletion on various cellular processes. Notably, depletion of these cellular polyamines resulted in a striking inhibition of translation initiation and cell growth. In the present study, we further investigated the effects of polyamine depletion on cell survival and apoptosis in AdSAT1-transduced 293T cells. Our results suggest that the depletion of both spermidine and spermine leads to apoptotic cell death in mammalian cells via the intrinsic mitochondrial pathway, as indicated by the changes in biochemical parameters, including loss of mitochondrial membrane potential, increase in pro-apototic Bax, decrease in anti-apoptotic Bcl-2, Bcl-xl and Mcl-1, and release of cytochrome c leading to caspase 3 activation and PARP cleavage. The morphological changes shown in the transmission electron microscopy (TEM) images, including nuclear fragmentation, cell shrinkage, vacuolization, mitochondrial alteration and membrane blebbing further illustrate apoptotic cell death upon depletion of cellular polyamines. Growth arrest and apoptosis of AdSAT1-transduced cells could be reversed by the addition of the stable polyamine analogs, α-methylspermidine (α-MeSpd), and N^1,N^{12}-dimethylspermine (Me_2Spm), that are not substrates for SAT1, supporting the notion that depletion of spermidine and spermine leads to apoptotic cell death.

EXPERIMENTAL

Materials

Precast NuPAGE (bisTris) gels and associated buffers, Click-iT TUNEL kit, Alexa Flour 488 secondary antibody, Prolong gold antifade reagent, LIVE/DEAD cell imaging kit and Annexin-V FITC/propidium iodide were purchased from Life Technologies. Cell counting kit (CCK-8) was purchased from Dojindo laboratories, Japan. The SAT1 antibody was purchased from Santa Cruz Biotechnology, Inc. Cleaved PARP, Bcl-2, Bcl-xl, Mcl-1, Bax

antibodies were from Cell Signaling. JC-1 (5,5′,6,6′-Tetrachloro-1,1′3,3′-tetraethyl-imidacarbocyanine iodide) kit and eIF5A antibody were procured from BD Biosciences. Formaldehyde, 4′, 6′-diamidino-2-phenylindole (DAPI), MDL 72527 (N^1, N^4-Bis(2,3-butadienyl)-1,4-butanediamine hydrochloride), cycloheximide and N-Acetyl-L-cysteine (NAC) were from Sigma-Aldrich. Cytochrome c antibody and cell fractionation kit was from Abcam. Enzchek caspase 3 assay kit was purchased from Molecular Probes. AdGFP and custom synthesized AdSAT1 viruses were procured from Signagen Laboratories. N^1, N^{11}-bis(ethyl)norspermine (BENSpm) was kindly provided by Dr. Patrick Woster (University of Medicine South Carolina) and α-methyl spermidine (α-MeSpd) and N^1,N^{12}-dimethylspermine (Me_2Spm) were kindly provided by Drs. Tuomo A. Keinänen (University of Eastern Finland, Kuopio, Finland) and Alex R. Khomutov (Russian Academy of Sciences, Moscow, Russia). A rabbit polyclonal antibody specific for hypusinated form of eIF5A [27] was a generous gift from Dr. Raghavendra Mirmira (Indiana University).

Methods

Cell Culture and Adenoviral Transduction—HEK293T (or 293T) cells were cultured in DMEM supplemented with 10% heat-inactivated FBS. For transduction, cells were trypsinized and resuspended (2×10^5 cells/ml) in DMEM media containing 10% FBS. AdGFP or AdSAT1 virus was added to the cell suspension at the multiplicity of infection (MOI) of 20. After mixing the cells with virus for 30 min, they were seeded in tissue culture dishes.

Determination of Cellular Polyamine Contents—HEK293T cells (six-well plate) were washed with ice cold PBS twice, harvested, and precipitated with 0.1 ml cold 10% (vol/vol) TCA. 50 μl of the TCA supernatant was used for polyamine analysis by ion exchange chromatographic system as described [28]. TCA precipitate was dissolved in 0.05 ml of 0.1 N NaOH and an aliquot was used for protein determination using Bradford Assay.

Cell viability and proliferation Assays—Cell death was assessed using the LIVE/DEAD cell imaging kit, according to manufacturer's instructions. Briefly, untransduced or transduced cells were plated in 96-well plates (0.5×10^4 cells per well in 0.1 ml medium) and treated as indicated. At 24, 48 and 72 h, cells were stained by adding 0.1 ml of live-green and dead-red dye mixture (2X) and incubated for 20 min at 25 °C. The media was removed and live imaging solution was added and images were taken using an Axiophot epiflourescence microscope (Zeiss). Cell proliferation was measured using Cell Counting Kit-8 (CCK-8), a sensitive colorimetric assay kit to determine levels of cell viability. Cells, untransduced or transduced with adenovirus, were seeded in 96-well plates (0.3×10^4 cells per well). At the indicated time points, 10 μl of the Cell Counting Kit-8 solution containing water-soluble tetrazolium salt (WST-8) was added to each well and cells were incubated at 37 °C for 2 h. Cell numbers were estimated by measuring the absorbance at a wavelength of 450 nm in a 96-well format plate reader (Microplate Reader, Perkin Elmer).

Annexin V and propidium iodide (PI) Fluorescent Activated Cell Sorter (FACS) analyses—Cells were analyzed for phosphatidylserine exposure by the annexin-V FITC/propidium iodide double-staining method according to the manufacturer's instructions. 293T

cells, untransduced or transduced with AdSAT1 or treated with cycloheximide (1 μg/ml) for the indicated periods, were washed with PBS, harvested by gentle trypsinization, (combined with floating cells washed with PBS) and resuspended in annexin-binding buffer at ~1 × 10^6 cells/ml. 5 μl of Alexa Fluor® 488 annexin V (Component A) and 1 μl of propidium iodide solution (100 μg/ml in annexin-binding buffer) were added to 100 μl of cell suspension and cells were incubated at room temperature for 15 minutes. Then 400 μl of annexin-binding buffer was added and the samples were kept on ice prior to flow cytometry (Fortessa).

Terminal Uridine Nucleotide End Labeling (TUNEL) assay—TUNEL assay was performed using the Click-iT® TUNEL Alexa Fluor® 594 Imaging Assay kit, according to the manufacturer's instructions. Briefly, cells untreated, or transduced with AdGFP or AdSAT1 were washed with PBS and fixed in 4% formaldehyde for 15 min followed by permeabilization in 0.25% Triton X-100 for 20 min. Then fluorescent labeling was performed by the addition of the Click-IT reaction mixtures. For counter-immuno-staining, the cells, after TUNEL assay, were incubated with primary anti-SAT1 antibody followed by the Alexa fluor 488 secondary antibody.

Measurement of Caspase 3 Activity—The cellular activity of caspase 3-like proteases was determined using Enzchek caspase 3 assay kit according to the manufacturer's protocol with minor modifications. Each cell sample (1 × 10^6 cells) was resuspended in 50 μl of cell lysis buffer and the mixture was incubated on ice for 30 min and vortexed for 10 min. After centrifugation (5000 ×g, 4° C, 5 min), 50 μl of the supernatant fluid were added into the wells of a 96-well plate and 50 μl working solution was added to each well and incubated at room temperature for 30 minutes. Fluorescence was measured at 342 nm (excitation) and at 441 nm (emission) using a SPECTRAmax® 190 microplate photometer (Molecular Devices).

Analysis of mitochondrial integrity using JC-1 dye—Mitochondrial membrane potential in untransduced and AdSAT1-transduced HEK 293T cells was estimated using the flow cytometry analysis method for JC-1 probe. Briefly, 1 × 10^6 cells were suspended in 500 μl of 1X JC-1 solution (10 μg/ml) and incubated at 37°C for 15 min. Cells were then centrifuged at 1000 ×g for 5 min and washed twice with 1 X assay buffer and analyzed immediately using a flow cytometer (Fortessa). Data was collected using 488-nm excitation with 530nm and 590 nm emission filters.

Separation of the mitochondrial fraction—Cytosolic and mitochondrial fractions were separated using a cell fractionation kit (Abcam) according to manufacturer's instructions.

Transmission Electron Microscopy (TEM)—TEM was performed by the NCI Frederick core facility and adherent cultured cells in 6-well plate were embedded and processed by the *in situ* method described previously [29].

RESULTS

SAT1 overexpression causes depletion of spermidine and spermine and reduces viability in HEK293T cells

The polyamine content of AdSAT1-transduced cells compared with those of untransduced or AdGFP-transduced cells (Table 1) shows that the levels of spermidine and spermine were reduced to less than 10 % of the control level (those in untransduced cells) by 24 h of AdSAT1 transduction and decreased further upon prolonged incubation (24–72 h). The polyamine content in AdGFP-transduced cells was similar to those in untransduced cells. Time-dependent, high accumulation of N^1-acetylspermidine and putrescine, the products of SAT1- and APAO-mediated polyamine catabolism, was observed in AdSAT1-transduced cells, but not in untransduced or AdGFP-transduced cells (Table 1). The sum of the accumulated products of polyamine oxidation, putrescine and N^1-acetylspermidine, in AdSAT1-transduced cells exceeded the sum of spermidine and spermine in control cells, probably due to the continued supply of SAT1 substrates, *i.e*. newly synthesized spermidine and spermine, in these cells.

The effects of SAT1 overexpression on growth and viability were examined and compared with other samples, including untransduced, cycloheximide- and DFMO-treated samples (Fig. 1), using a LIVE/DEAD cell imaging kit. Live cells exhibit a green color due to conversion of the non-fluorescent, cell-permeant calcein to the fluorescent calcein by intracellular esterase activities. Dying and dead cells exhibit red fluorescence due the DNA binding of the dead-red dye, which can enter cells only when the plasma membrane is damaged. At all the time points, but especially with increasing time, the fraction of dead/dying cells was much higher in the AdSAT1-transduced samples than in the untransduced samples (Fig. 1). As AdSAT1 transduction can cause a pronounced inhibition of protein synthesis [9], we compared the effects of AdSAT1-transduction with those of cycloheximide treatment. Cell death was much less in samples treated with cycloheximide (1 μg/ml, the concentration that was estimated to inhibit protein synthesis by >80%) than in AdSAT1-transduced samples. As DFMO depletes cellular putrescine and spermidine but not spermine, its effects were also compared. While cell growth was gradually inhibited by DFMO treatment, cell death was far less in these samples than in AdSAT1-transduced samples. Interestingly, the AdSAT1-transduced cells displayed rounder morphology with reduced lamellipodia by 24 h of transduction, consistent with the previous reports [23], but such changes in cell attachment or morphology were not observed in the cycloheximide- or DFMO-treated cells.

To check the possibility that the high levels of N^1-acetylspermidine and putrescine accumulated in AdSAT1-transduced cells (Table 1) exert deleterious effects on cells, we tested these compounds. However, addition of these compounds (5 mM) to medium, alone (Fig. 1) or in combination (not shown), did not cause inhibition of growth or loss of viability. We also tested three polyamine analogs, α- MeSpd, Me_2Spm and BENSpm, that could support protein synthesis in AdSAT1-transduced 293T cells [9] for their ability to restore viability. α-MeSpd and Me_2Spm increased the number of viable cells and reduced cell death, but BENSpm did not.

Inhibition of growth and loss of viability in AdSAT1-transduced cells is due to depletion of spermidine and spermine

We then investigated the underlying mechanism of growth inhibition in SAT1-overexpressing cells by measuring cell viability and growth using a quantitative colorimetric assay (Cell Counting Kit-8) (Fig. 2A–2D). AdSAT1 transduction led to an arrest of growth by 24 h and a loss of viable cells during the 24–72 h period (Fig. 2A), whereas AdGFP-transduction caused a relatively small inhibition of growth. The growth inhibition in DFMO-treated cells was less pronounced than in AdSAT1-transduced cells, probably because cellular spermine is not depleted upon DFMO-treatment (Table 1). As cell death in certain cases of SAT1 induction was attributed to oxidative stress resulting from accelerated polyamine catabolism, we examined the effects of MDL 72527, an inhibitor of APAO and SMO. This compound alone (at 100 and 300 μM) did not restore the growth of AdSAT1-transduced cells (Fig. 2B). Furthermore, addition of N-Acetyl-cysteine (NAC), a commonly used anti-oxidant, at 1–10 mM did not reverse growth inhibition in AdSAT1-transduced cells (Fig. 2C), suggesting that the growth inhibition and cell death upon AdSAT1-transduction are not due to oxidative stress. Then, we wondered whether the growth inhibition in AdSAT1-transduced cells could be due to deprivation of acetyl-CoA resulting from a polyamine metabolic flux. Metabolic flux was reported to occur in certain mammalian cells [24, 30] or a SAT1 transgenic animal [31], when the polyamine biosynthetic enzymes, ODC and AdoMetDC, are highly induced to counteract the enhanced polyamine catabolism by overexpressed SAT1, thereby setting up a futile cycle of biosynthesis and degradation with consumption of two AcCoA and one ATP per cycle. In the AdSAT1-transduced cells, SAT1 superinduction was transient (Fig. 2E) and there were no significant changes in ODC enzyme level (Fig. 2E). Moreover, growth of AdSAT1-transduced cells was not restored upon addition of DFMO (Fig. 2B), unlike in the SAT1-overexpressing LNCaP cells in which DFMO restored cell growth by blocking the polyamine futile cycle [24]. These findings suggest that growth arrest in these AdSAT1-transduced cells is not due to the metabolic flux-related energy deprivation.

The effects of the polyamine analogs α-MeSpd, Me_2Spm and BENSpm on cell growth of untransduced and AdSAT1-transduced cells were measured (Fig. 2D). Consistent with the data from Live/Dead cell imaging in Fig 1, α-MeSpd and Me_2Spm partially restored the growth, suggesting that the growth arrest in AdSAT1-transduecd cells is attributable to the depletion of spermidine and spermine in these cells. Although BENSpm, as a polycation, is able to promote protein synthesis [9], it could not restore cell growth (Fig. 2D). This finding implies an as yet unknown, critical function of the natural polyamines, in addition to hypusine synthesis, that cannot be fulfilled by BENSpm.

We previously reported that eIF5A could be acetylated and inactivated by SAT1 *in vitro* [32]. In order to determine whether the growth inhibition in AdSAT1-transduced cells could be due to a decrease in the level of active eIF5A, hypusinated eIF5A levels were measured, using a hypusine-specific antibody [27] that recognizes eIF5A containing hypusine or deoxyhypusine, but not the unmodified lysine form nor the acetylhypusinated form (Fig. 3A). There was no significant reduction in the hypusinated eIF5A level in AdSAT1-transduced cells up to 72 h (Fig. 3B). Given that eIF5A is an abundant and stable protein

with a long half-life, it is not probable that a small reduction in hypusinated eIF5A results in the growth arrest of these AdSAT1-transduced cells.

AdSAT1-transduction causes apoptosis by an intrinsic mitochondrial pathway

We employed several methods to determine whether cell death in AdSAT1-transduced cells occurs by apoptosis. Annexin V/PI FACS analyses showed a clear rise in early and late apoptotic cells after 24–72 h of AdSAT1 transduction compared to untransduced cells (Fig. 4A). In untransduced samples, the percentages of early apoptotic cells (annexin V positive, PI negative, green, right lower block) and late apoptotic cells (annexin V positive, PI positive, orange color, right upper block) were low at all the time points. In the AdSAT1-transduced samples, the early and late apoptotic cells as well as dead cells (annexin V negative, PI positive, red color, upper left block) were markedly increased. Reciprocally, the percent of healthy cells (black, annexin V negative, PI negative) was much lower in AdSAT1-transduced samples (47.3–75.3%) than in untransduced samples (~90%). Addition of MDL 72527 did not make a significant difference in apoptosis at 48–72 h of AdSAT1 transduction (sum of early, late apoptotic and dead cells in Fig. 4A and dead cell proportion in Fig. 1). Thus, apoptosis in AdSAT1-transduced cells appears to be largely due to depletion of spermidine and spermine, rather than due to oxidative stress. Cycloheximide treatment caused relatively small increases in early and late apoptotic cells compared to AdSAT1 transduction.

The TUNEL assay also revealed an increase in DNA fragmentation in SAT1-overexpressing cells (Fig. 4B, white arrows) at 48 h of AdSAT1 transduction. Increased nuclear fragmentation was also detected in these cells by DAPI staining (Fig. 4B, white arrows). Caspase 3 activity was significantly increased in AdSAT1-transduced cells, compared to untransduced and AdGFP-transduced cells at 24–72 h of transduction (Fig. 4C). In contrast to AdSAT1-transduced cells, no or little DNA or nuclear fragmentation was observed in AdGFP-transduced cells (Fig. 4B), and there were only small increases in caspase 3 over untransduced cells (Fig. 4C), suggesting that the apoptosis is primarily due to SAT1 overexpression but not due to adenoviral infection.

The mechanism of apoptosis in AdSAT1-transduced cells was investigated by analyzing mitochondrial membrane potential, Bcl-2 family proteins and cytochrome c release (Fig 5). The electrochemical gradient across the mitochondrial inner membrane is critical for normal mitochondrial function. Opening of the permeability transition pore in the inner mitochondrial membrane disrupts mitochondrial transmembrane potential ($\Delta\Psi m$). In order to determine whether AdSAT1-induced apoptosis is mitochondria-mediated, we measured the mitochondrial membrane potential using JC-1 dye by the flow cytometry analysis. In this experiment, mitochondrial depolarization is indicated by a decrease in the ratio of red to green fluorescence. 293T cells transduced with AdSAT1 displayed a marked drop in this ratio after 24–72 h of transduction (Fig. 5A), suggesting a loss of mitochondrial membrane potential, while little change was observed in untransduced cells.

The levels of Bcl-2 family members, proposed regulators of mitochondrial membrane potential and permeability [33], were examined by western blotting. In AdSAT1-transduced cells, pro-apoptotic Bax level was markedly enhanced, whereas the levels of anti-apoptotic

markers, Bcl-2, Bcl-xl and Mcl-1 were much reduced, compared to untransduced or AdGFP-transduced cells (Fig 5B). Loss of ΔΨm and mitochondrial outer membrane permeabilization leads to release of cytochrome c. As expected, we observed the release of cytochrome c from mitochondria to cytoplasm concomitant with a decrease in the mitochondrial fraction in AdSAT1-transduced cells (Fig. 5C).

Transmission Electron Microscopy (TEM) of AdSAT1-transduced cells

TEM images (Fig. 6) of untransduced cells (at 48 h) showed intact cells with large nuclei, numerous golgi apparatus, many smooth endoplasmic reticulums and mitochondria. Cells with certain morphological changes associated with apoptosis [34] increased after 24 h of AdSAT1 transduction. At 24–72 h of AdSAT1-transduction, morphological changes, including membrane blebbing, nuclear fragmentation, abnormal mitochondria and cell shrinkage were seen. These cells also contained a large number of vacuoles and lipid bodies in the cytoplasm and the cytoplasm density was lighter than that of the controls. At 72 h of AdSAT1 transduction, degenerated or swollen mitochondria with reduced cristae were clearly visible. Lipid bodies (LB) could be observed in AdSAT1-transduced cells at 48 and 72 h of transduction. Lipid bodies were reported to form in apoptotic cells when fatty acid β-oxidation is inhibited by mitochondrial dysfunction [35]. The AdGFP-transduced cells showed an increase in vacuoles at 48 h, but did not show other apoptotic features, suggesting that apoptosis in the AdSAT1-transduced cells was mainly caused by an over-expression of SAT1 rather than by the adenoviral transduction.

DISCUSSION

The rapid and extensive depletion of spermidine and spermine by AdSAT1 transduction has permitted us to examine the direct effects of polyamine depletion and to address the role of polyamines in cell growth, viability and apoptosis. The current data demonstrate that the depletion of spermidine and spermine leads to apoptosis in 293T cells through the intrinsic mitochondrial pathway, as evidenced by various biochemical markers, such as loss of mitochondrial membrane potential, changes in Bcl-2 family proteins and release of cytochrome c leading to activation of caspase 3 and PARP cleavage. Annexin V and PI FACS analyses provided clear indication of apoptosis in AdSAT1-transduced cells and TEM images of AdSAT1-transduced cells revealed ultrastructural changes commonly associated with apoptosis. As we showed in earlier study [9] that an inhibition of protein synthesis accompanied growth inhibition, we wondered whether, or to what extent, the apoptosis in these cells is attributable to the inhibition of protein synthesis. Treatment with cycloheximide (1 μg/ml) caused only moderate apoptosis in 293T cells (Fig. 1 and 4A) compared to AdSAT1 transduction suggesting that apoptosis in AdSAT1-transduced cells is largely due to depletion of the polyamines spermidine and spermine.

Our work is distinct from SAT1 overexpression studies by others, in that a transient super-induction of SAT1 (Fig. 2E) and nearly total depletion of spermidine and spermine are achieved within 24 h of AdSAT1 transduction (Table 1). Thus, adenoviral overexpression of SAT1 offered us a unique window of opportunity to address the causal relationship between depletion of these polyamines and cellular effects. Previous SAT1 overexpression studies

involved selection of stable cell clones after transfection with a non-inducible [26] or an inducible SAT1 expression vector [23–25]. In these other studies, SAT1 induction was not as great nor as rapid as in our study and depletion of spermidine and/or spermine was not extensive, because of the compensatory induction of the polyamine biosynthetic enzymes, ODC and AdoMetDC, an apparent adaptation response by the cells. Under such circumstances, growth inhibition could not be attributed solely to a reduction in cellular polyamines. For example, in a LNCaP cell clone harboring an inducible SAT1 vector, growth arrest upon induction of SAT1 expression was attributed mainly to AcCoA deprivation resulting from futile cycles of biosynthesis and degradation [24, 30]. In contrast, polyamine metabolic flux does not appear to be involved in growth inhibition of AdSAT1-transduced cells, because there was no significant increase of the ODC enzyme level in the AdSAT1-transduced cells (Fig. 2E) and because DFMO did not restore cell growth (Fig. 2B). In our system, in which SAT1 induction is transient (probably due to its short half-life and inhibition of new synthesis of SAT1), a futile metabolic cycle dependent on maintenance of elevated levels of both biosynthetic and catabolic enzyme activities, could not be established.

Activation of the polyamine catabolic pathway has been implicated in tissue damage associated with various pathological conditions including cancer, kidney failure, inflammation, stroke and diabetes, through generation of H_2O_2, reactive aldehydes or acrolein [36]. For example, SAT1 induction has been associated with ischemia/reperfusion injury of kidney, and the tissue damage could be ameliorated by MDL 72527, an inhibitor of APAO and SMO [37], suggesting an oxidative stress-mediated mechanism. The same mechanism of apoptosis was also inferred in breast cancer cell lines in which growth inhibition from a high induction of SAT1 and SMO, by treatment with BENSpm, was alleviated by MDL 72527 [38]. We have also considered oxidative stress as a potential mechanism of growth inhibition in AdSAT1-transduced cells. However, the polyamine oxidase inhibitor, MDL 72527, or an antioxidant, NAC, did not restore growth of AdSAT1-transduced cells (Fig. 2B and Fig. 2C) and MDL72527 did not significantly reduce apoptosis of AdSAT1-transduced cells (Fig. 4A), suggesting that oxidative stress from accelerated polyamine catabolism is not responsible for the growth arrest and apoptotic cell death.

In our earlier study, we showed that the inhibition of translation in AdSAT1-transduced cells could be reversed by the addition of polyamine analogs, such as BENSpm, α-MeSpd or Me_2Spm, that are not substrates for SAT1 [9]. α-MeSpd, and Me_2Spm have been reported to substitute for natural polyamines in supporting long-term growth of certain mammalian cells in the presence of DFMO [39], or in the presence of an inhibitor of AdoMetDC [40] and in preventing acute pancreatitis in the SAT1 transgenic rat [41]. The ability to sustain long term growth in the absence of natural spermidine was attributed to the ability of α-MeSpd to act as a substrate for hypusine synthesis [40, 42] and the ability of Me_2Spm to be converted to α-MeSpd. In accordance with these results, we observed that α-MeSpd and Me_2Spm could also restore growth (Fig. 2D) and prevent apoptosis of AdSAT1-transduced cells (Fig. 1) suggesting that, in fact, it is the depletion of spermidine and spermine that causes growth arrest and apoptosis. Although BENSpm could support protein synthesis in AdSAT1-transduced 293T cells [9], nevertheless, unlike α-MeSpd and Me_2Spm, it could not restore cell growth (Fig. 2D) nor could it prevent apoptosis. This finding suggests that there are

other critical processes that are fulfilled by the natural polyamines but not by BENSpm. In fact, BENSpm alone can induce apoptosis in various human cancer cell lines in a cell type-specific manner [38], through induction of SAT1 and SMO1, and down-regulation of the polyamine biosynthetic enzymes, ODC and AdoMetDC, or through as yet unknown mechanisms. Although a similarly high induction of SAT1 and depletion of polyamines can be accomplished using BENSpm, the SAT1 overexpression by AdSAT1 transduction differs from BENSpm-induced SAT1 overexpression in that it does not involve side effects of BENSpm.

Apoptosis in AdSAT1-transduced 293T cells bears a certain analogy to apoptotic cell death and mitochondrial dysfunction of a *Sacchromyces cerevisiae* mutant (Δ*spe*2) with deletion of the gene encoding AdoMetDC, the enzyme required for synthesis of spermidine and spermine [43]. This mutant strain has a high level of cellular putrescine but lacks endogenous spermidine and spermine and thus depends on a supply of spermidine in the medium for growth. The mutant is especially sensitive to oxidative stress [44] and undergoes intrinsic mitochondrial apoptotic cell death in the absence of spermidine supplementation, suggesting that polyamines are important for the maintenance and stability of mitochondrial membranes.

Furthermore, the loss in the mitochondrial membrane potential, changes in Bcl-2 family proteins, release of cytochrome c and altered mitochondria ultrastructure in AdSAT1-transduced cells indicate apoptotic cell death through a mitochondria-mediated pathway. Polyamines bind to mitochondrial surface phospholipids, owing to the strong affinity of the basic amines for these lipids. The resultant charge neutralization may result in a membrane that is less permeable or mechanically stronger [45] and it is known that spermine binding inhibits membrane permeability transition in isolated mitochondria [46]. Moreover, spermine was reported to prevent cytochrome c release in glucocorticoid-induced apoptosis in mouse thymocytes [47]. Taken together, our data provide strong evidence that polyamine depletion by AdSAT1 transduction induces apoptosis through the intrinsic pathway mediated by mitochondrial alterations. The AdSAT1 virus used in this study exhibits potent effects *i.e.* complete depletion of spermidine and spermine and total arrest in cell growth with ensuing apoptotic cell death. Our studies lay a foundation upon which to develop a tumor specific, oncolytic virus overexpressing SAT1.

Acknowledgments

We thank Edith C. Wolff [National Institute of Dental and Craniofacial Research (NIDCR) National Institutes of Health (NIH)] for helpful suggestions on manuscript. The research was supported by intramural research program of NIDCR, NIH.

FUNDING

The research was supported by the intramural program of the National Institute of Dental and Craniofacial Research, National Institutes of Health.

Abbreviations used

SAT1 (or an alternate abbreviation, SSAT1)	spermidine/spermine-N^1-acetyltransferase-1
AdSAT1	SAT1-encoding adenovirus
AdGFP	GFP-encoding adenovirus
ODC	ornithine decarboxylase
APAO	acetylpolyamine oxidase
SMO	spermine oxidase
DFMO	α-difluoromethylornithine
AdoMetDC	adenosylmethionine decarboxylase
GFP	green fluorescent protein
eIF5A	eukaryotic translation initiation factor 5A
BENSpm	N^1, N^{11}-bis(ethyl)norspermine
α-MeSpd	α-methylspermidine
Me2Spm	N^1, N^{12}-dimethylspermine
EM	electron microscopy
TEM	transmission electron microscopy
FACS	fluorescent activated cell sorter
PARP	Poly ADP ribose polymerase
PI	propidium iodide
AcCoA	acetyl coenzyme A
NAC	N-Acetyl-L-cysteine

References

1. Pegg AE. Mammalian polyamine metabolism and function. IUBMB Life. 2009; 61:880–894. [PubMed: 19603518]
2. Pegg AE, Casero RA Jr. Current status of the polyamine research field. Methods Mol Biol. 2011; 720:3–35. [PubMed: 21318864]
3. Tabor CW, Tabor H. Polyamines. Annu Rev Biochem. 1984; 53:749–790. [PubMed: 6206782]
4. Igarashi K, Kashiwagi K. Modulation of cellular function by polyamines. Int J Biochem Cell Biol. 2010; 42:39–51. [PubMed: 19643201]
5. Gerner EW, Meyskens FL Jr. Polyamines and cancer: old molecules, new understanding. Nat Rev Cancer. 2004; 4:781–792. [PubMed: 15510159]
6. Rial NS, Meyskens FL, Gerner EW. Polyamines as mediators of APC-dependent intestinal carcinogenesis and cancer chemoprevention. Essays Biochem. 2009; 46:111–124. [PubMed: 20095973]
7. Nowotarski SL, Woster PM, Casero RA Jr. Polyamines and cancer: implications for chemotherapy and chemoprevention. Expert Rev Mol Med. 2013; 15:e3. [PubMed: 23432971]

8. Park MH, Nishimura K, Zanelli CF, Valentini SR. Functional significance of eIF5A and its hypusine modification in eukaryotes. Amino Acids. 2010; 38:491–500. [PubMed: 19997760]
9. Mandal S, Mandal A, Johansson HE, Orjalo AV, Park MH. Depletion of cellular polyamines, spermidine and spermine, causes a total arrest in translation and growth in mammalian cells. Proc Natl Acad Sci U S A. 2013; 110:2169–2174. [PubMed: 23345430]
10. Seiler N, Raul F. Polyamines and apoptosis. J Cell Mol Med. 2005; 9:623–642. [PubMed: 16202210]
11. Spotheim-Maurizot M, Ruiz S, Sabattier R, Charlier M. Radioprotection of DNA by polyamines. Int J Radiat Biol. 1995; 68:571–577. [PubMed: 7490507]
12. Ha HC, Sirisoma NS, Kuppusamy P, Zweier JL, Woster PM, Casero RA Jr. The natural polyamine spermine functions directly as a free radical scavenger. Proc Natl Acad Sci U S A. 1998; 95:11140–11145. [PubMed: 9736703]
13. Agostinelli E, Arancia G, Vedova LD, Belli F, Marra M, Salvi M, Toninello A. The biological functions of polyamine oxidation products by amine oxidases: perspectives of clinical applications. Amino Acids. 2004; 27:347–358. [PubMed: 15592759]
14. Sharmin S, Sakata K, Kashiwagi K, Ueda S, Iwasaki S, Shirahata A, Igarashi K. Polyamine cytotoxicity in the presence of bovine serum amine oxidase. Biochem Biophys Res Commun. 2001; 282:228–235. [PubMed: 11263996]
15. Fong LY, Nguyen VT, Pegg AE, Magee PN. Alpha-difluoromethylornithine induction of apoptosis: a mechanism which reverses pre-established cell proliferation and cancer initiation in esophageal carcinogenesis in zinc-deficient rats. Cancer Epidemiol Biomarkers Prev. 2001; 10:191–199. [PubMed: 11303587]
16. Nitta T, Igarashi K, Yamamoto N. Polyamine depletion induces apoptosis through mitochondria-mediated pathway. Exp Cell Res. 2002; 276:120–128. [PubMed: 11978014]
17. Ploszaj T, Motyl T, Zimowska W, Skierski J, Zwierzchowski L. Inhibition of ornithine decarboxylase by alpha-difluoromethylornithine induces apoptosis of HC11 mouse mammary epithelial cells. Amino Acids. 2000; 19:483–496. [PubMed: 11128555]
18. Zou C, Vlastos AT, Yang L, Wang J, Nishioka K, Follen M. Effects of difluoromethylornithine on growth inhibition and apoptosis in human cervical epithelial and cancerous cell lines. Gynecol Oncol. 2002; 85:266–273. [PubMed: 11972386]
19. Bhattacharya S, Ray RM, Johnson LR. Role of polyamines in p53-dependent apoptosis of intestinal epithelial cells. Cell Signal. 2009; 21:509–522. [PubMed: 19136059]
20. Bhattacharya S, Ray RM, Viar MJ, Johnson LR. Polyamines are required for activation of c-Jun NH2-terminal kinase and apoptosis in response to TNF-alpha in IEC-6 cells. Am J Physiol Gastrointest Liver Physiol. 2003; 285:G980–991. [PubMed: 12869386]
21. Ray RM, Viar MJ, Yuan Q, Johnson LR. Polyamine depletion delays apoptosis of rat intestinal epithelial cells. Am J Physiol Cell Physiol. 2000; 278:C480–489. [PubMed: 10712236]
22. Pegg AE. Spermidine/spermine-N(1)-acetyltransferase: a key metabolic regulator. Am J Physiol Endocrinol Metab. 2008; 294:E995–1010. [PubMed: 18349109]
23. Wang Z, Zahedi K, Barone S, Tehrani K, Rabb H, Matlin K, Casero RA, Soleimani M. Overexpression of SSAT in kidney cells recapitulates various phenotypic aspects of kidney ischemia-reperfusion injury. J Am Soc Nephrol. 2004; 15:1844–1852. [PubMed: 15213272]
24. Kee K, Vujcic S, Merali S, Diegelman P, Kisiel N, Powell CT, Kramer DL, Porter CW. Metabolic and antiproliferative consequences of activated polyamine catabolism in LNCaP prostate carcinoma cells. J Biol Chem. 2004; 279:27050–27058. [PubMed: 15096507]
25. Vujcic S, Halmekyto M, Diegelman P, Gan G, Kramer DL, Janne J, Porter CW. Effects of conditional overexpression of spermidine/spermine N1-acetyltransferase on polyamine pool dynamics, cell growth, and sensitivity to polyamine analogs. J Biol Chem. 2000; 275:38319–38328. [PubMed: 10978316]
26. McCloskey DE, Coleman CS, Pegg AE. Properties and regulation of human spermidine/spermine N1-acetyltransferase stably expressed in Chinese hamster ovary cells. J Biol Chem. 1999; 274:6175–6182. [PubMed: 10037702]
27. Nishiki Y, Farb TB, Friedrich J, Bokvist K, Mirmira RG, Maier B. Characterization of a novel polyclonal anti-hypusine antibody. Springerplus. 2013; 2:421. [PubMed: 24024105]

28. Folk JE, Park MH, Chung SI, Schrode J, Lester EP, Cooper HL. Polyamines as physiological substrates for transglutaminases. J Biol Chem. 1980; 255:3695–3700. [PubMed: 6102569]
29. Gonda MA, Aaronson SA, Ellmore N, Zeve VH, Nagashima K. Ultrastructural studies of surface features of human normal and tumor cells in tissue culture by scanning and transmission electron microscopy. J Natl Cancer Inst. 1976; 56:245–263. [PubMed: 1255758]
30. Kramer DL, Diegelman P, Jell J, Vujcic S, Merali S, Porter CW. Polyamine acetylation modulates polyamine metabolic flux, a prelude to broader metabolic consequences. J Biol Chem. 2008; 283:4241–4251. [PubMed: 18089555]
31. Jell J, Merali S, Hensen ML, Mazurchuk R, Spernyak JA, Diegelman P, Kisiel ND, Barrero C, Deeb KK, Alhonen L, Patel MS, Porter CW. Genetically altered expression of spermidine/spermine N1-acetyltransferase affects fat metabolism in mice via acetyl-CoA. J Biol Chem. 2007; 282:8404–8413. [PubMed: 17189273]
32. Lee SB, Park JH, Folk JE, Deck JA, Pegg AE, Sokabe M, Fraser CS, Park MH. Inactivation of eukaryotic initiation factor 5A (eIF5A) by specific acetylation of its hypusine residue by spermidine/spermine acetyltransferase 1 (SSAT1). Biochem J. 2011; 433:205–213. [PubMed: 20942800]
33. Cory S, Huang DC, Adams JM. The Bcl-2 family: roles in cell survival and oncogenesis. Oncogene. 2003; 22:8590–8607. [PubMed: 14634621]
34. White MK, Cinti C. A morphologic approach to detect apoptosis based on electron microscopy. Methods Mol Biol. 2004; 285:105–111. [PubMed: 15269403]
35. Boren J, Brindle KM. Apoptosis-induced mitochondrial dysfunction causes cytoplasmic lipid droplet formation. Cell Death Differ. 2012; 19:1561–1570. [PubMed: 22460322]
36. Park MH, Igarashi K. Polyamines and their metabolites as diagnostic markers of human diseases. Biomol Ther (Seoul). 2013; 21:1–9. [PubMed: 24009852]
37. Zahedi K, Barone S, Wang Y, Murray-Stewart T, Roy-Chaudhury P, Smith RD, Casero RA Jr, Soleimani M. Proximal tubule epithelial cell specific ablation of the spermidine/spermine N1-acetyltransferase gene reduces the severity of renal ischemia/reperfusion injury. PLoS One. 2014; 9:e110161. [PubMed: 25390069]
38. Pledgie A, Huang Y, Hacker A, Zhang Z, Woster PM, Davidson NE, Casero RA Jr. Spermine oxidase SMO(PAOh1), Not N1-acetylpolyamine oxidase PAO, is the primary source of cytotoxic H2O2 in polyamine analogue-treated human breast cancer cell lines. J Biol Chem. 2005; 280:39843–39851. [PubMed: 16207710]
39. Jarvinen A, Grigorenko N, Khomutov AR, Hyvonen MT, Uimari A, Vepsalainen J, Sinervirta R, Keinanen TA, Vujcic S, Alhonen L, Porter CW, Janne J. Metabolic stability of alpha-methylated polyamine derivatives and their use as substitutes for the natural polyamines. J Biol Chem. 2005; 280:6595–6601. [PubMed: 15611107]
40. Byers TL, Lakanen JR, Coward JK, Pegg AE. The role of hypusine depletion in cytostasis induced by S-adenosyl-L- methionine decarboxylase inhibition: new evidence provided by 1-methylspermidine and 1,12-dimethylspermine. Biochem J. 1994; 303:363–368. [PubMed: 7980394]
41. Hyvonen MT, Herzig KH, Sinervirta R, Albrecht E, Nordback I, Sand J, Keinanen TA, Vepsalainen J, Grigorenko N, Khomutov AR, Kruger B, Janne J, Alhonen L. activated polyamine catabolism in acute pancreatitis: alpha-methylated polyamine analogues prevent trypsinogen activation and pancreatitis-associated mortality. Am J Pathol. 2006; 168:115–122. [PubMed: 16400014]
42. Hyvonen MT, Keinanen TA, Cerrada-Gimenez M, Sinervirta R, Grigorenko N, Khomutov AR, Vepsalainen J, Alhonen L, Janne J. Role of hypusinated eukaryotic translation initiation factor 5A in polyamine depletion-induced cytostasis. J Biol Chem. 2007; 282:34700–34706. [PubMed: 17901051]
43. Balasundaram D, Tabor CW, Tabor H. Oxygen toxicity in a polyamine-depleted spe2 delta mutant of Saccharomyces cerevisiae. Proc Natl Acad Sci U S A. 1993; 90:4693–4697. [PubMed: 8506320]

44. Chattopadhyay MK, Tabor CW, Tabor H. Polyamine deficiency leads to accumulation of reactive oxygen species in a spe2Delta mutant of Saccharomyces cerevisiae. Yeast. 2006; 23:751–761. [PubMed: 16862607]

45. Tabor H, Tabor CW. Spermidine, Spermine, and Related Amines. Pharmacol Rev. 1964; 16:245–300. [PubMed: 14211123]

46. Lapidus RG, Sokolove PM. Spermine inhibition of the permeability transition of isolated rat liver mitochondria: an investigation of mechanism. Arch Biochem Biophys. 1993; 306:246–253. [PubMed: 8215411]

47. Hegardt C, Andersson G, Oredsson SM. Spermine prevents cytochrome c release in glucocorticoid-induced apoptosis in mouse thymocytes. Cell Biol Int. 2003; 27:115–121. [PubMed: 12662968]

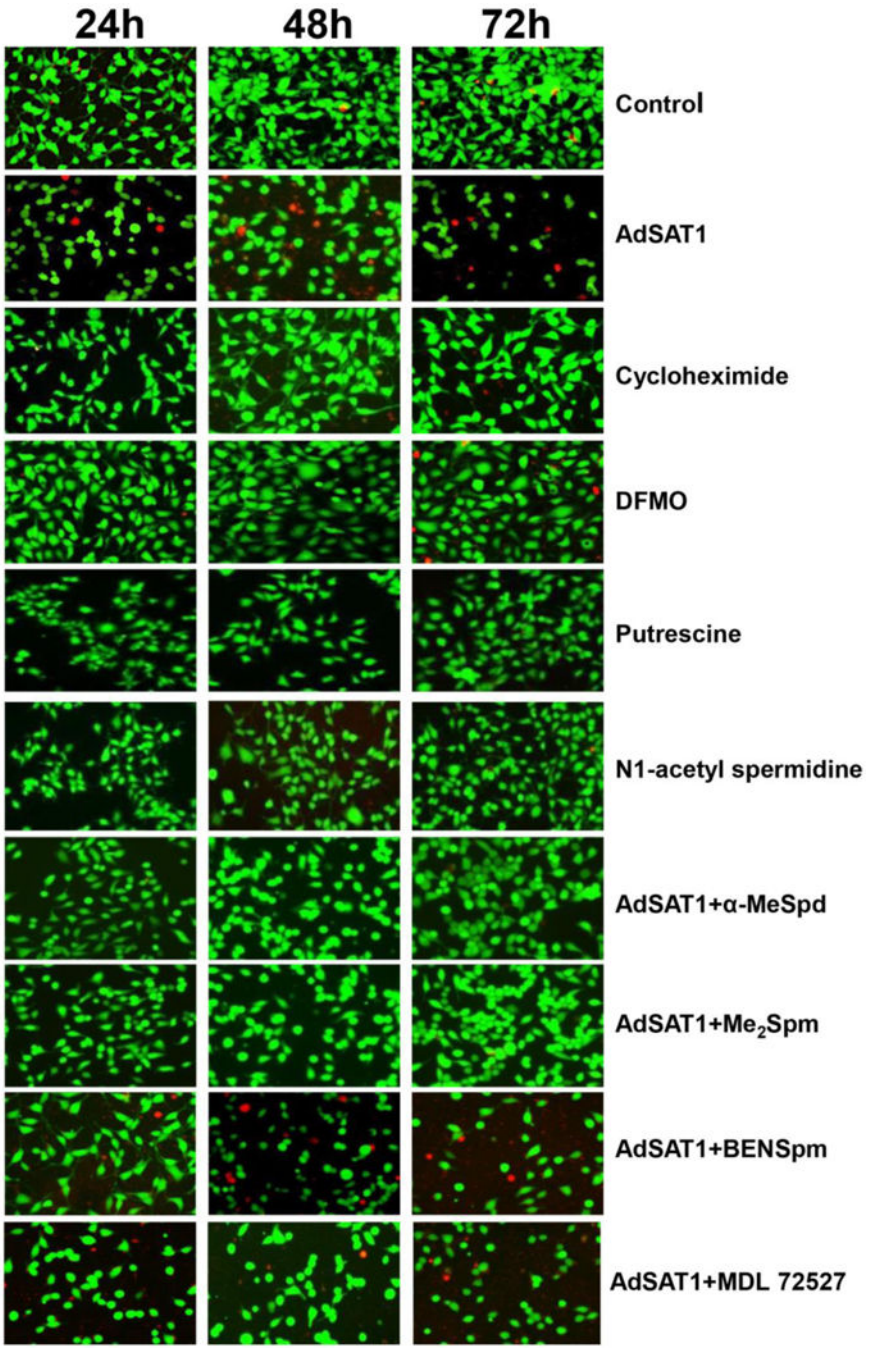

FIGURE 1. Effects of AdSAT1 transduction, cycloheximide, DFMO, putrescine, N^1-acetylspermidine, α-MeSpd, Me_2Spm and BENSpm on cell viability

Viability of 293T cells was examined using a Live/dead cell imaging kit at 24, 48 and 72 h after seeding with no treatment (control), or AdSAT1 transduction, or treatment with cycloheximide (1 μg/ml), or with DFMO (5 mM), putrescine (5 mM) or N^1-acetylspermidine (5 mM) or AdSAT1 transduction with added BENSpm (10 μM), α-MeSpd (100 μM), Me_2Spm (100 μM). The concentrations of BENSpm, α-MeSpd and Me_2Spm were chosen based on previous reports [9, 42]. Cells were stained with calcein and dead-red to visualize live and dead cells, respectively. Live cells fluoresce a bright green, whereas

dead cells with damaged membranes fluoresce a red color. Representative images from three independent experiments are shown.

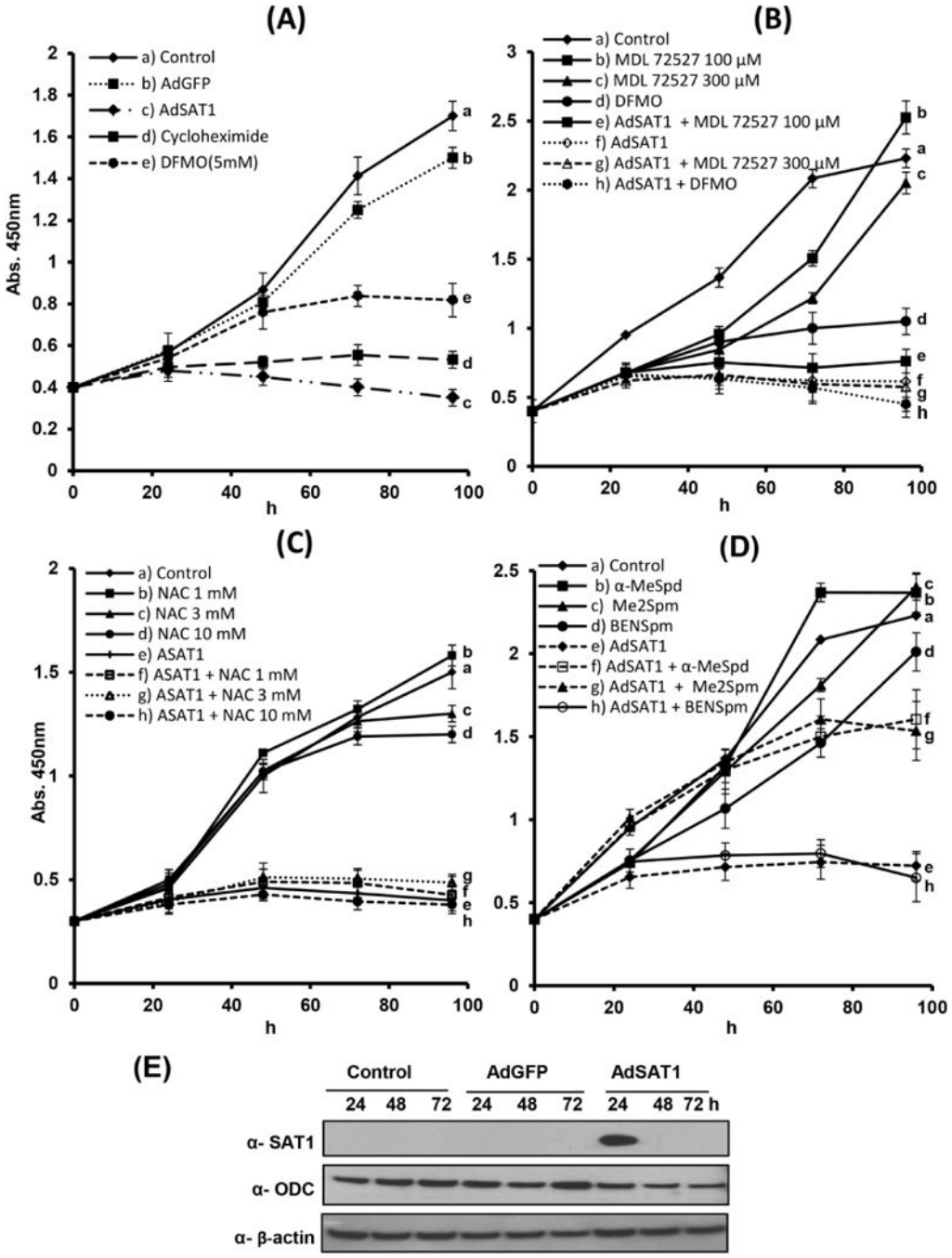

FIGURE 2. Effects of various compounds on the growth and the levels of SAT1 and ODC in untransduced, AdGFP-transduced and AdSAT1-transduced 293T cells

The compounds were added to the culture medium at the time of seeding and cell growth was monitored using Cell Counting Kit-8 (CCK-8) as described under Experimental Procedures. Average values from two independent experiments carried out in triplicate were plotted. (**A**) effects of AdGFP transduction, AdSAT1 transduction, or DFMO (5 mM) treatment on 293T cell growth. (**B**) effects of MDL 72527 (100 µM and 300 µM) and DFMO(5 mM) on the growth of untransduced or AdSAT1-transduced 293T cells. (**C**)

effects of N-Acetyl-cysteine (NAC) on growth of untransduced and AdSAT1-transduced 293T cells. *D*, α-MeSpd (100 μM), Me_2Spm (100 μM), or BENSpm (10 μM) on the growth of untransduced or AdSAT1-transduced cells. *E*, The time course of SAT1 and ODC protein levels were examined by western blotting.

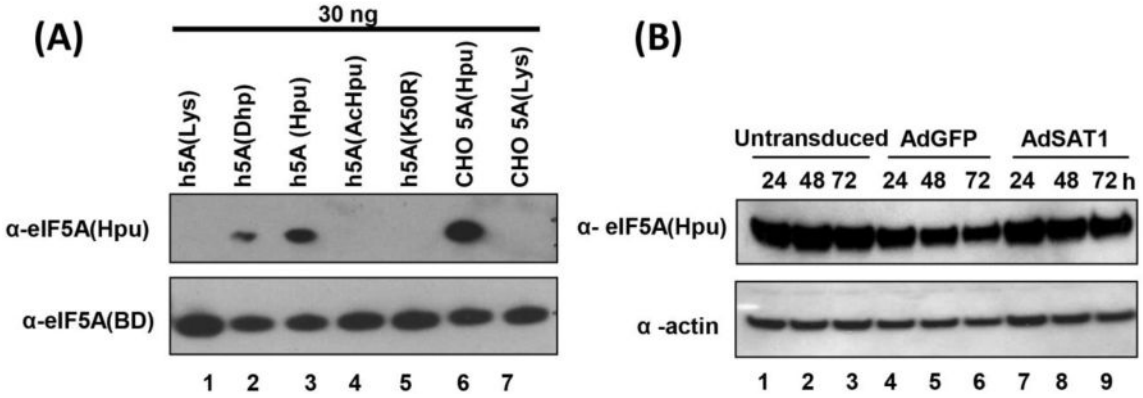

FIGURE 3. Specificity of the hypusine-specific eIF5A antibody and effect of SAT1 overexpression on the hypusinated eIF5A levels

(**A**) Purified eIF5A proteins of various forms were tested using the hypusine-specific eIF5A antibody (top panel) [27] or eIF5A antibody (BD Biosciences) that recognizes all eIF5A forms (bottom panel). Lanes 1–3, recombinant human eIF5A containing lysine, deoxyhypusine or hypusine at residue 50. Lane 4, purified, acetylated eIF5A obtained by acetylation of recombinant human eIF5A(Hpu) using SAT1, lane 5, recombinant human eIF5A K50R mutant protein, lane 6, endogenous hypusine- containing eIF5A purified from CHO cells. Lane 7, unmodified eIF5A precursor isolated from DFMO-treated CHO cells. (**B**) Cell lysates from untransduced, AdGFP-transduced and AdSAT1-transduced 293T cells harvested at indicated times were analyzed using hypusine-specific eIF5A antibody verified in **A**. Abbreviations are: h5A(Lys), human eIF5A containing Lys at 50th residue; h5A(Dhp), human eIF5A containing deoxyhypusine; h5A(Hpu), human eIF5A containing hypusine; h5A(AcHpu), human eIF5A containing acetylhypusine; h5A(K50R), human eIF5A containing Arg at 50th residue.

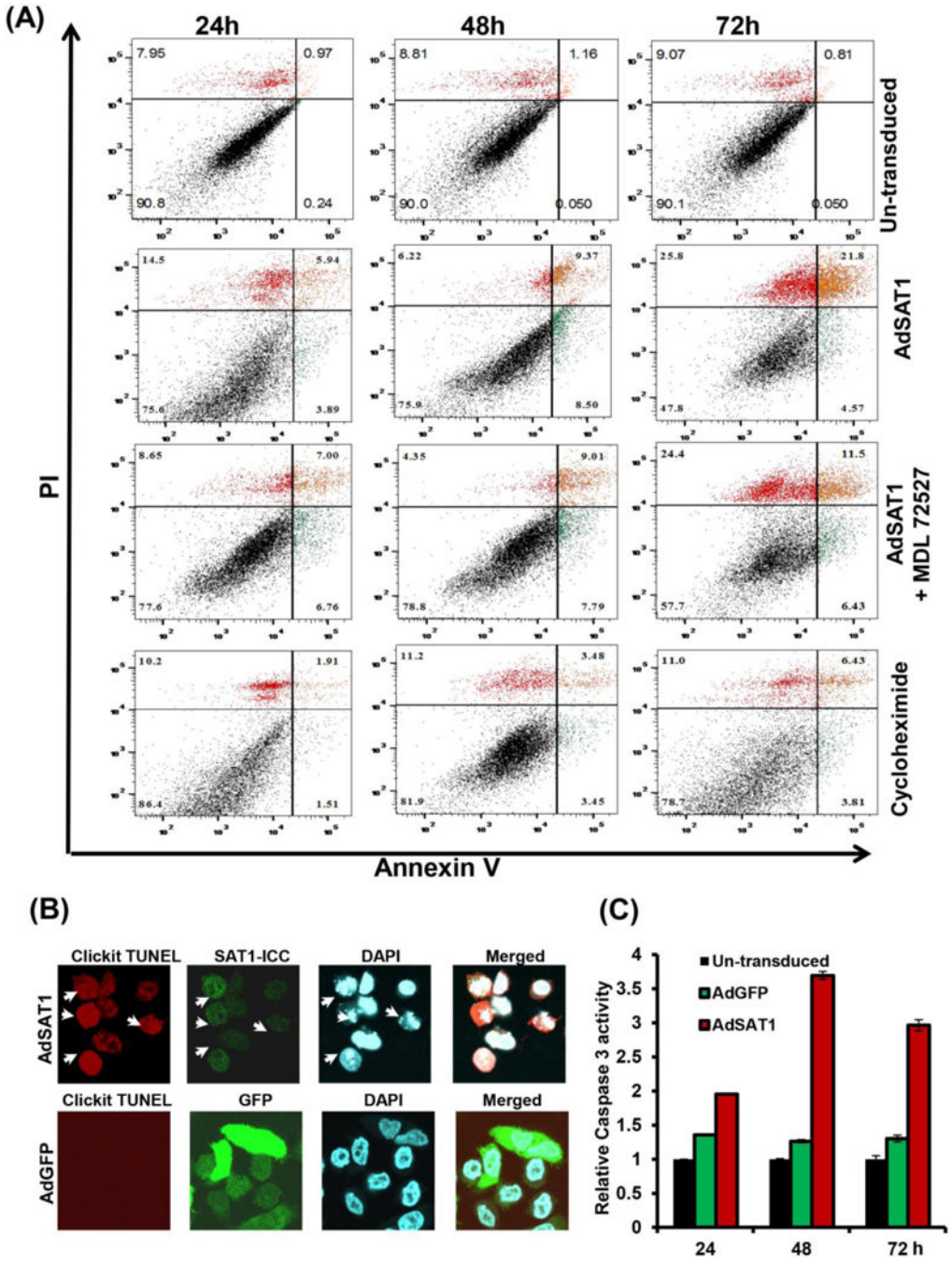

FIGURE 4. Annexin V/PI FACS analyses, TUNEL assay and caspase 3 assay of AdSAT1-transduced and control 293T cells

(**A**) Apoptosis was measured at 24, 48 and 72 h of treatment by FACS analyses using Annexin V-FITC/PI double staining. 100 μM of MDL72527 or 1 μg/ml of cycloheximide was added to the sample as indicated. The percentage of apoptotic cells was calculated from fluorescence dot plots using quadrant statistics (10,000 cells/experiment). One representative experiment is shown. (**B**) Cells transduced with AdSAT1 or AdGFP were fixed and stained for the TUNEL assay at 48 h as described in Experimental Procedures. After the TUNEL

assay, SAT1 immunocytochemistry (SAT1-ICC) was performed. The arrows indicate TUNEL positive cells which coincide with those with high expression of SAT1 and those with nuclear fragmentation upon staining with DAPI. The photomicrographs are representative images from three independent experiments. (**C**) Caspase 3 activity was measured as described under “Methods” with cell lysates prepared at 24 h, 48 h and 72 h of transduction. Bar graphs show data (mean ± SD) from three independent experiments done in duplicate.

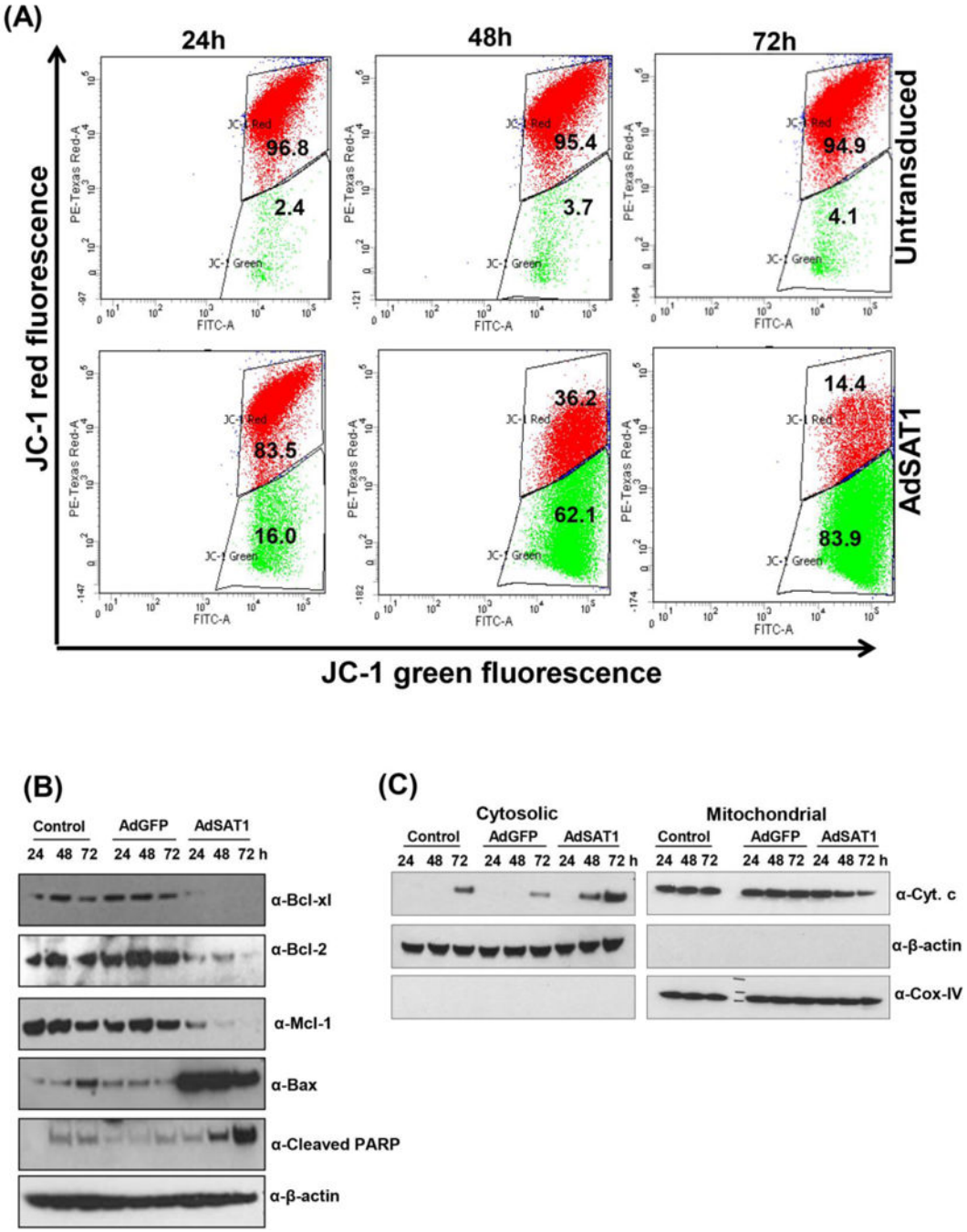

FIGURE 5. Analyses of mitochondrial membrane potential, western blotting of apoptosis markers and cytochrome c release

(**A**) Untransduced and AdSAT1-transduced cells were stained with the mitoprobe JC-1 dye as described under Experimental Procedures. Red fluorescence represent cells with normal mitochondria membrane potential and green fluorescence represent those with depolarized mitochondrial membrane. Experiments were carried out twice in duplicates with 30,000 cells per analysis. One representative data is shown. (**B**) changes in the levels of apoptotic marker proteins in untransduced, AdGFP- or AdSAT1-transduced cells. (**C**) Western blot

analyses of cytochrome c in the cytosol and mitochondrial fractions at different time points after adenoviral transduction. β-actin and Cox-IV were used as markers for cytoplasm and mitochondria, respectively.

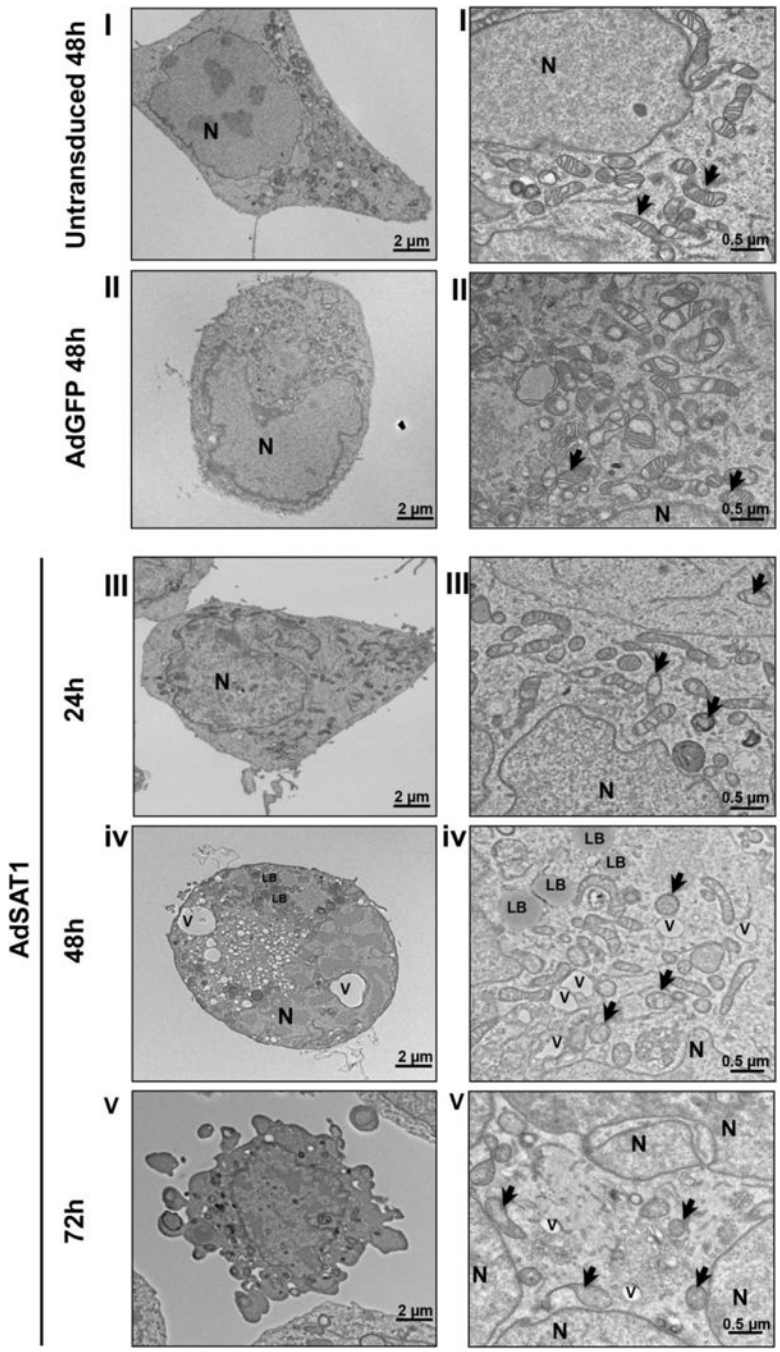

FIGURE 6. Transmission electron microscopy of untransduced, AdGFP-transduced and AdSAT1-transduced 293T cells

TEM was performed on thin sections of 293T cells, untransduced at 48 h (panel set I), AdGFP-transduced at 48 h (Panel set II) or AdSAT1-transduced at 24, 48 and 72 h (panel sets III, IV and V, respectively). The images on the right side are at higher magnification. Mitochondria are indicated by arrows, nucleus by N, vacuole by V and lipid body by LB. Representative images are shown.

Table 1

The effects of transduction with AdGFP or AdSAT1 or DFMO treatment on cellular polyamine contents.

Sample		N^1-Acetyl Spermidine	Putrescine	Spermidine	Spermine
	hours			(nmol/mg protein)	
Untrans.	24	n.d.	2.2 ± 0.5	12.83 ± 1.1	11.2 ± 0.65
	48	n.d.	n.d.	10.17 ± 0.96	15.27 ± 1.92
	72	n.d.	n.d.	8.03 ± 0.46	15.5 ± 1.07
AdGFP	24	n.d.	3.08 ± 0.8	10.1 ± 0.78	12.5 ± 0.60
	48	n.d.	n.d.	9 ± 1.13	11.6 ± 0.92
	72	n.d.	n.d.	8.5 ± 1.20	15.6 ± 0.76
AdSAT1	24	47.4 ± 2.5	18 ± 1.28	1.1 ± 0.05	0.48 ± 0.04
	48	36.3 ± 1.63	16.3 ± 1.56	0.63 ± 0.03	0.2 ± 0.08
	72	32.3 ± 1.54	14 ± 1.11	n.d.	n.d.
DFMO	24	n.d.	n.d.	2 ± 0.86	12.5 ± 0.53
	48	n.d.	n.d.	0.5 ± 0.29	10 ± 1.6
	72	n.d.	n.d.	0.2 ± .04	9.5 ± 1.39

293T cells were untransduced or transduced with AdGFP or AdSAT1, or treated with DFMO (5 mM). At 24, 48 and 72 h after transduction or treatment, cells were washed with PBS, harvested and cellular polyamines were extracted with 10% TCA and polyamines were analyzed as described under Experimental Procedures. The values (nmol/mg protein) are expressed as mean ± S.D.

n.d. = not detectable where the limit of detection was 0.1 nmol/mg protein.